Molecular Dynamics Study of Ion Capture from Water by a Model Ionophore, Tetraprotonated Cryptand SC24

Brian Owenson,[†] Robert D. MacElroy,[†] and Andrew Pohorille*[,‡]

Contribution from NASA Ames Research Center, Moffett Field, California 94035, and the Department of Chemistry, University of California, Berkeley, California 94720.
Received March 7, 1988

Abstract: A molecular dynamics study of chloride capture from water by the tetraprotonated cryptand SC24 is presented. The system under study consisted of a cryptand molecule, chloride ion, and 319 water molecules. Calculations were performed for 19 distances between the cryptand and the chloride. For each distance a trajectory of at least 60 ps was obtained. Two anion binding sites of comparable energy were found. The chloride can bind either inside the cryptand cavity or more loosely outside of the ligand. The binding sites are separated by an energy barrier of 20 kcal/mol. Chloride movement toward the cryptand is accompanied by stepwise dehydration of the anion. The energy loss due to this dehydration is offset by the electrostatic attraction between the anion and the ligand and by an increase in favorable water-water interactions. The most striking feature of chloride capture is a rapid cooperative change in the conformation of the cryptand when the Cl^- starts to enter the ligand and just as it encounters the energy barrier. The conformational transition is associated with a shift of three N-H bonds from the pure endo orientation, so that they point toward the chloride. The shift provides electrostatic stabilization, which compensates for the loss of the remaining three water molecules from the hydration shell of the anion. The N-H bonds remain directed toward the anion during its further movement into the ligand and guide chloride into a stable position inside the cryptand cavity. The flexibility of the receptor, the stepwise dehydration of an ionic substrate, and the characteristic balance between different energy components in the system all may be features of ion binding common to a wide range of abiotic and biological ionophores.

Efficient and selective transport of ions across membranes is essential for proper cell function. The process of removing ions from the aqueous environment and transferring them across a nonpolar membrane interior usually requires some assistance, which is provided by specialized ionophores that are either ion channels[1] or mobile ion carriers.[2] For both types of ionophores the efficiency and the selectivity of ion transport is determined to a significant extent by the initial step in which the ion undergoes partial or complete dehydration and moves into direct contact with the ionophore. Expenditure of the energy required for dehydration must be compensated, at least in part, by an energy gain from favorable substrate-ligand interactions. Even though different ionophores have widely different molecular structures, it is expected that there are common general features characterizing the mechanisms by which the ionophores bind ions. Identifying and understanding these features would greatly add to our knowledge about ion transport.

Biological ionophores are complex molecules, usually peptides with many conformational degrees of freedom. One strategy for studying the general principles of ion binding is to turn to a group of less complex, abiotic receptors. These molecules can efficiently and selectively bind ions, and some of them have sufficient lipophilic character to transport ions across membranes.[3] A special class of ionophores that recently has attracted much attention are the macrocyclic receptors (cryptands).[4] Cryptands can bind cations or anions with high strength and selectivity to form inclusion complexes (cryptates), in which the ion is located inside the molecular cavity. One of the simplest and best characterized ligands is the spherical macrotricycle SC24.[5,6] This cryptand is constructed of four nitrogen atoms located in the vertices of a tetrahedron and linked with six CH_2-CH_2-O-CH_2-CH_2 bridges. Inside this molecule is a cavity that can accommodate an ionic substrate. The cryptand exhibits an interesting feature that at basic or neutral pHs it selectively binds NH_4^+;[5] however, when it is triprotonated or tetraprotonated at low pHs, it preferentially binds Cl^-.[6]

In this report we present a molecular dynamics study of chloride capture from water by the tetraprotonated cryptand, shown in Figure 1. The main objectives of this work were (i) to calculate energetic changes that occur during anion capture, (ii) to identify structural properties of the cryptand that facilitate the capture, and (iii) to obtain a molecular level description of rearrangements of water structure that result from ion dehydration. The calculations were performed with two primary conditions on the mechanism of ion binding by the cryptand.

The first condition was that all four N-H bonds at the vertices of the free cryptand were set to the endo conformation. This means that the bonds were oriented pointing into the ligand cavity, as in the crystal structure of the cryptate.[7] NMR spectra of free cryptand molecules suggest that the dominant form at room temperature is such that two N-H bonds are oriented exo (pointing away from the cavity). However, at elevated temperatures populations of other conformers markedly increase, as demonstrated by the increase in proton exchange rates.[6] At $T = 319$ K, at which these calculations were performed, the populations of the all endo and of the mixed endo-exo conformers of the cryptand become similar.

The second condition was that binding of Cl^- occurs only with the tetraprotonated form of the cryptand. A possibility that complex dissociation is preceded by deprotonation at pH values close to the $pK_4 = 2.2$[6] was not considered. However, as our recent results suggest,[8] the mechanism of chloride capture by the triprotonated and the tetraprotonated cryptand should be similar.

[†] NASA Ames Research Center.
[‡] University of California, Berkeley.

(1) For recent reviews, see: Eisenman, G.; Dani, J. A. *Annu. Rev. Biophys. Biophys. Chem.* **1987**, *16*, 205. Yellen, G. *Ibid.* **1987**, *16*, 227. Begenisich, T. *Ibid.* **1987**, *16*, 247. Tsien, R. W.; Hess, P.; McCleskey, E. W.; Rosenberg, R. L. *Ibid.* **1987**, *16*, 265.

(2) Simon, W.; Morf, W. E.; Meier, P. Ch. *Struct. Bonding (Berlin)* **1973**, *16*, 113. Ovchinnikov, Yu. A.; Ivanov, V. T.; Shkrob, A. M. *Membrane-Active Complexons*; Elsevier: Amsterdam, The Netherlands, 1974. Dobler, M. *Ionophores and Their Structures*; Wiley: New York, 1981.

(3) Lehn, J. M. In *Physical Chemistry of Transmembrane Ion Motions*; Spach, G., Ed.; Elsevier: New York, 1983; pp 181-206. Grimaldi, J. J.; Lehn, J. M. *J. Am. Chem. Soc.* **1979**, *101*, 1333. Hriciga, A.; Lehn, J. M. *Proc. Natl. Acad. Sci. U.S.A.* **1983**, *80*, 6426.

(4) Lehn, J. M. *Struct. Bonding (Berlin)* **1973**, *16*, 1. Lehn, J. M. *Pure Appl. Chem.* **1978**, 50, 871. Lehn, J. M. *Science (Washington, D.C.)* **1985**, *227*, 849.

(5) Graf, E.; Kintzinger, J. P.; Lehn, J. M.; LeMoigne, J. *J. Am. Chem. Soc.* **1982**, *104*, 1672.

(6) Kintzinger, J. P.; Lehn, J. M.; Kauffmann, E.; Dye, J. L.; Popov, A. I. *Ibid.* **1983**, *105*, 7549.

(7) Metz, B.; Rosalsky, J. M.; Weiss, R. *J. Chem. Soc., Chem. Commun.* **1976**, 533.

(8) Owenson, B.; MacElroy, R. D.; Pohorille, A. *THEOCHEM*, in press.

0002-7863/88/1510-6992$01.50/0

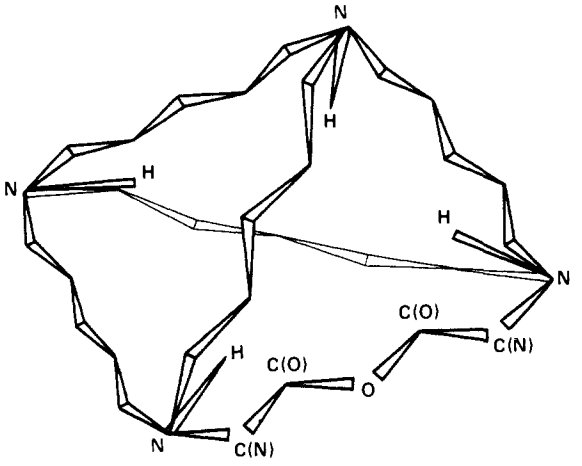

Figure 1. Structure of the tetraprotonated cryptand SC24. Hydrogen atoms bonded to carbon atoms are not shown.

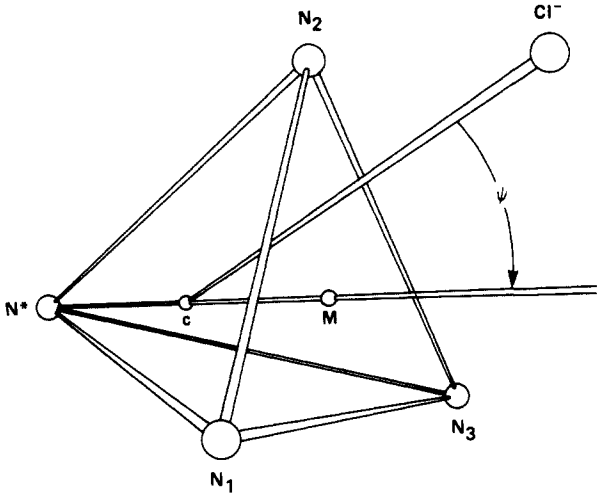

Figure 2. Schematic representation of r_c. The cryptand is represented as a tetrahedron with nitrogen atoms in the vertices. The chloride ion approaches a face of the cryptand formed by nitrogen atoms N_i (i = 1–3). N* is the nitrogen atom farthest away from the Cl^-. M is the midpoint of a triangle formed by the nitrogen atoms N_i. The center of the cryptand, c, lies on the N*–M line, 3 Å from the N*. The c–Cl distance is the value of the coordinate r_c. Angle ψ is formed between the N*–c–M line and r_c.

Methods

Description of the System. The system under study consisted of a tetraprotonated cryptand molecule, one chloride ion, and 319 water molecules enclosed in a cube with an edge length of 21.73 Å. Standard periodic boundary conditions were applied. The initial geometry of the cryptand was taken from crystallographic data on its complex with Cl^-.[7] The number of water molecules was chosen such that water density beyond the region immediately influenced by the cryptand was approximately equal to that of bulk water.

Because of the tetrahedral symmetry of the cryptand, chloride capture can be considered as a process in which the anion enters the ligand cavity through one of four equivalent faces formed by three nitrogen atoms and three CH_2–CH_2–O–CH_2–CH_2 bridges. The behavior of the system was monitored as a function of ion position along a coordinate r_c, defined as the distance between the ion and the center of the cryptand. The center of the cryptand was defined as a point located 3 Å from the nitrogen atom farthest from the chloride and lying on a line joining this nitrogen atom with the midpoint of the triangle formed by the remaining three nitrogen atoms. This definition was chosen because it provides a stable reference point in the flexible cryptand and because it takes advantage of the symmetry of the system. A schematic representation of the coordinate r_c is shown in Figure 2.

Intermolecular Potential Functions. Water–water interactions were represented by the TIP4P model potential.[9] A potential function developed by Jorgensen,[10] which uses the same description of a water molecule, was employed to describe interactions between water and chloride, and the potential function proposed by Hagler et al.[11] was used for calculating water–cryptand interactions and the intrinsic energy of the cryptand.

Table I. Parameters for Calculating Potential Energy between Cl^- and Cryptand[a]

atom	q	c, kcal/mol·Å^{12}	d, kcal/mol·Å^6	p, kcal/mol·Å^4
N	+0.172	3 764 400	2683.7	461.68
C(N)	+0.195	1 486 500	590.3	
C(O)	+0.165	3 602 700	340.6	
O	−0.414	1 115 400	1705.3	276.12
H(C)	+0.021	2 356	207.8	
H(N)	+0.117			

[a] Parameter α for nonadditive interactions is equal to 1108.4 kcal/mol·Å^4.

Since intermolecular potentials describing interactions between cryptand and chloride were not available, we performed a series of quantum mechanical calculations on model systems to obtain such potentials. These model systems consisted of a chloride ion and molecules similar to fragments of the cryptand. Potential functions for interactions of the chloride with the oxygen atoms of the cryptand and the adjacent methylene groups were obtained from calculations on the chloride–dimethyl ether complex. Calculated energies of interaction between chloride and methyl-, dimethyl-, and trimethylammonium ions were used to evaluate potential functions for interactions of Cl^- with the remaining atoms of the cryptand. Of these model molecules, trimethylammonium ion most faithfully represents the environment of the cryptand nitrogen atoms. However, trimethylammonium is too large to explore reliably the entire potential energy surface for its interactions with Cl^-. Thus, energies of interaction between Cl^- and the other methylated derivatives were also included in the derivation of the potential functions.

The quantum mechanical results reported here were obtained by SCF molecular orbital calculations.[12] For the model molecules the 6-31G** basis set was used. A basis set with additional diffused polarization functions was employed for Cl^-. Dispersion energy was partially included by the MP2 perturbational procedure. For the system consisting of dimethyl ether and Cl^-, 50 points on the potential energy surface were calculated. The same total number of points was obtained for methylammonium ions and chloride. In the calculations the model molecules were kept fixed while the position of chloride was changed angularly and radially. Figure 3 shows the orientations of dimethyl ether and methylammonium ion in the coordinate system and presents the radial dependence of calculated energies of interactions between the model molecules and the chloride for several fixed angular orientations of Cl^-.

The accuracy of the computed energies was tested by extending the basis set to triple-ζ and by approximating the basis set superposition error for several typical configurations of the chloride around the model molecules. The extension of the basis set usually lowered the SCF energies of interaction by 0.5–2.0 kcal/mol. It also led to the increase in the contributions from electron correlation. The basis set superposition error estimated by the counterpoise method[13] was smaller than 1 kcal/mol. Although the total effect of the improvements in evaluating the energies of interaction was not negligible, the *relative* stabilities of different configurations were modified only slightly.

Strong electrostatic interactions between methylammonium ions and chloride raise the question of whether the commonly used pairwise additive approximation to intermolecular potentials is adequate in this case. To investigate this issue, we performed calculations on systems consisting of two, three, and four ammonium ions interacting with Cl^-. Ammonium ions were placed at the vertices of a tetrahedron separated by 5.5 Å, as in the cryptand. Chloride ion was placed in five different positions along the coordinate r_c defined above. It was found that the three-body effect for two ammonium ions interacting with the chloride located in the center of the tetrahedron was equal to 7.8 kcal/mol. On the other hand, four- and five-body contributions to the energies of interaction were much smaller (between −2.8 and −0.1 kcal/mol). Since the three-body effects appear to be large, we included them in our analytical formula for intermolecular potentials.

(9) Jorgensen, W. L.; Chandrasekhar, J.; Madura, J. D.; Impey, R. W.; Klein, M. L. *J. Chem. Phys.* **1983**, *79*, 926.

(10) Chandrasekhar, J.; Spellmeyer, D. C.; Jorgensen, W. L. *J. Am. Chem. Soc.* **1984**, *106*, 903.

(11) Hagler, A. T.; Moult, G.; Osguthorpe, D. *Biopolymers* **1980**, *19*, 395.

(12) The calculations were performed by an ab initio gradient program system GRADSCF designed and written by A. Komornicki at Polyatomics Research Institute.

(13) Boys, S. F.; Bernardi, F. *Mol. Phys.* **1970**, *19*, 553.

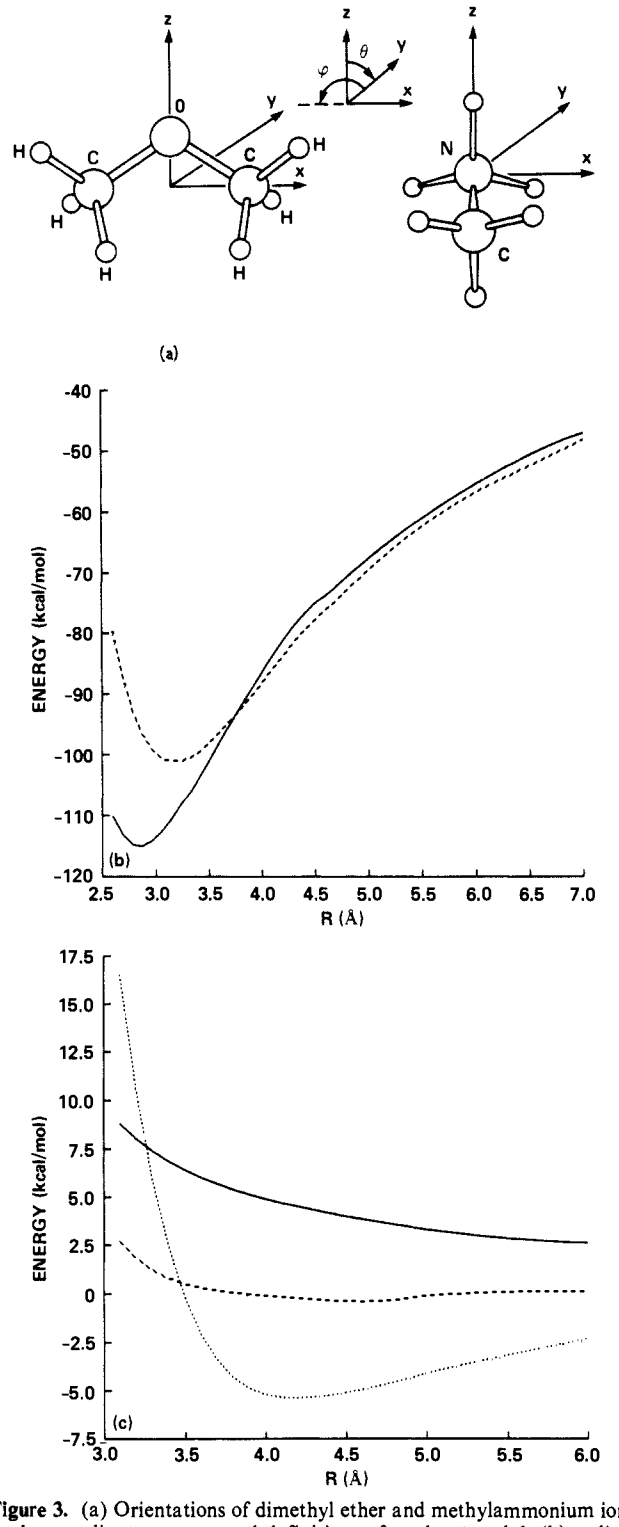

Figure 3. (a) Orientations of dimethyl ether and methylammonium ion in the coordinate system, and definitions of angles ϕ and θ; (b) radial dependence of calculated energies of interaction between methylammonium ion and chloride for ϕ, $\theta = 0°$, 0° (solid line) and ϕ, $\theta = 0°$, 45° (dashed line); and (c) radial dependence of calculated energies of interaction between dimethyl ether and chloride for ϕ, $\theta = 0°$, 0° (solid line), ϕ, $\theta = 90°$, 90° (dashed line), and ϕ, $\theta = 0°$, 135° (dotted line).

The calculated energies of interaction, E_{int}, were fitted to the following analytical formula for intermolecular potential functions:

$$E_{int} = \sum_i -332\left(\frac{q_i}{r_i} + \frac{c_i}{r_i^{12}} - \frac{d_i}{r_i^6} - \frac{p_i}{r_i^4}\right) - \sum_i \sum_{j \neq i} \frac{\alpha \cos(\phi_{N_i\text{-Cl-}N_j})}{r_i^2 r_j^2} \quad (1)$$

where r_i and r_j are the distances between the chloride and atoms i and j of the cryptand, $\phi_{N_i\text{-Cl-}N_j}$ is the angle formed by two nitrogen atoms, N_i and N_j, with Cl^-, and q_i, c_i, d_i, p_i, and α are adjustable parameters listed in Table I. The first term of eq 1, which describes the pairwise additive part of the intermolecular potentials, is a sum over all cryptand atoms. Parameters in this term were obtained by the least-squares fit of atom–atom potentials to the calculated energies of interactions in the dimers. The standard deviation was 1.0 kcal/mol for interactions of dimethyl ether with chloride and 1.6 kcal/mol for interactions between chloride and methylammonium ions. The second term in eq 1 is a sum over nitrogen atoms of the cryptand and describes three-body polarization effects. Parameter α in this term was obtained by a separate fit to the energies of interaction between two ammonium ions and chloride. To improve the reliability of this fit, results for 10 additional positions of Cl^- were also included.

Molecular Dynamics. Molecular dynamics calculations were performed for 19 different positions of the chloride along r_c evenly distributed between 0.2 and 5.6 Å. The equations of motion were integrated with the Verlet algorithm.[14] The SHAKE procedure[15] was applied to hold all C–H bond lengths rigid and to maintain the value of r_c.

All intermolecular interactions were smoothly truncated by Andersen's cutoff procedure.[16] For the water–chloride interactions the cutoff distances were equal to 7.5 and 8.0 Å. To evaluate the cryptand–water interactions, the cryptand molecule was divided into small groups. These groups were electrically neutral with the exception of four $NH(CH_2)_3$ groups, which carried a charge of 1e. The cutoff distances between each group and a water molecule were set to 6.5 and 7.0 Å. The same cutoff distances were applied to the water–water interactions. No cutoff distances were used for evaluating cryptand–chloride interactions.

For every value of r_c the system was aged until the desired temperature was reached and the potential energy stabilized. Typical aging times were 25–40 ps. The results reported here are based on a subsequent 60–100 ps of trajectory for each value of r_c. In all calculations the time step was 2 fs. The energy drift was less than 0.1%. In all runs we attempted to maintain a temperature of 319 K, which corresponds to the temperature at which most of experimental data on the cryptand were obtained.[6] However, actual temperatures varied by 2 K between runs. Statistical errors were estimated by assuming that averages over 5-ps time intervals are uncorrelated. Uncertainties given throughout this paper are ±1 standard deviation. All calculations presented here were performed on a Cray-2 supercomputer located at the Numerical Aerodynamic Simulator.

Results and Discussion

Total Energy Profile. In Figure 4a we show the calculated average potential energy of the system, U_{tot}, as a function of the chloride position along r_c. The energy curve exhibits two minima whose depths are identical within statistical error. One minimum, located at $r_c = 0.6$ Å corresponds to a position of the chloride inside the cavity of the cryptand and is narrow due to steric limitations imposed by the ligand. In contrast, the other minimum is broad and extends from $r_c = 2.6$ Å to $r_c = 5.0$ Å. In this minimum the chloride is located outside the cryptand, where it does not experience steric hindrance. Evidence that Cl^- binds outside of the cryptand also comes from the NMR studies.[6]

The two energy minima representing chloride inside and outside the cryptand are separated by a relatively flat energy barrier between $r_c = 1.1$ Å and $r_c = 2.6$ Å, which is approximately equal to 20 kcal/mol. This barrier corresponds to those configurations of the system in which the chloride passes through a face of the cryptand. The calculated height of the barrier is consistent with the experimentally measured activation energy for chloride binding of 16.2 kcal/mol.[6] Another region along r_c that exhibits increased energy is located at $r_c > 5.0$ Å and is due to the reduction of electrostatic attraction between the ligand and the chloride. For large values of r_c, beyond the range studied in this work, U_{tot} should increase as $1/r_c$.

Additional information that characterizes the energy minima was obtained from calculations in which the chloride was placed initially either inside or outside the cryptand and was then allowed to move without restrictions along r_c. In each run a trajectory of 75 ps was computed after equilibration. Because a substantial barrier exists between the two energy minima, the Cl^- remained in each case in the minimum to which it was initially assigned.

(14) Verlet, L. *Phys. Rev.* **1967**, *159*, 98.
(15) Ryckaert, J. P.; Ciccotti, G.; Berendsen, H. J. C. *J. Comput. Phys.* **1977**, *23*, 327.
(16) Andrea, T. A.; Swope, W. C.; Andersen, H. C. *J. Chem. Phys.* **1983**, *79*, 4577.

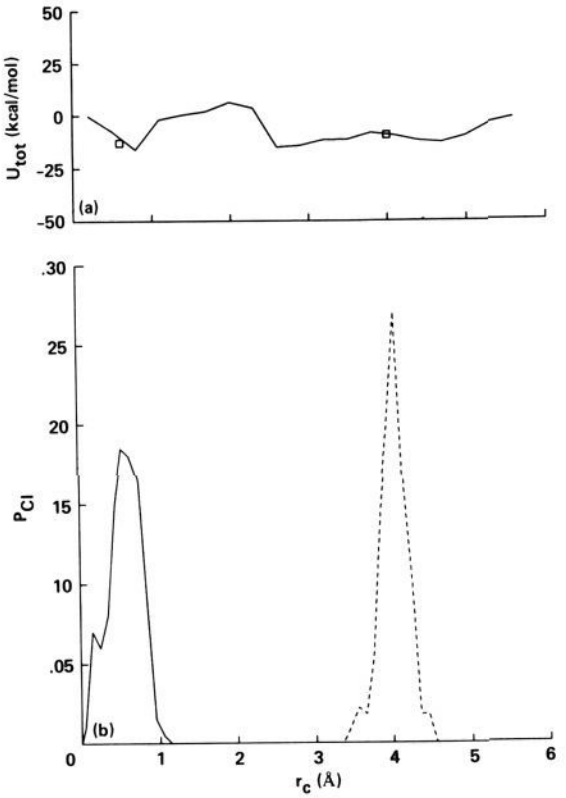

Figure 4. (a) Total potential energy U_{tot} of the system as a function of chloride position along r_c; (b) the probability distribution function, P_{Cl}, of finding Cl^- along r_c for the anion initially placed inside the cryptand (solid curve) and outside the cryptand (dashed line). White squares represent U_{tot} for both calculations. The energy curve was shifted such that the energy at r_c = 0.2 Å is equal to zero. Statistical uncertainties in U_{tot} are typically ±5 kcal/mol.

The average potential energies obtained from the two calculations correspond closely to the minima in the energy profile presented in Figure 4a. As shown in Figure 4b, the probability distribution functions for finding the chloride ion inside or outside the cryptand are centered at r_c = 0.8 Å and r_c = 4.0 Å, respectively, and both are approximately 1 Å wide. This result is at odds with the energy curve, shown in Figure 4a, which implies that the probability distribution function for finding the Cl^- in the cavity of the ligand should be much narrower than the probability distribution function of finding the Cl^- outside the cryptand. The unexpected breadth of the probability distribution for finding the Cl^- in the cavity may be due to the entropic factors, not discussed in this work. Another possible explanation is that during the calculations in which r_c is fixed the movement of the system on the potential energy surface is restricted by energy barriers due to steric hindrance between the cryptand and the anion. On the other hand, if the chloride is allowed to move freely along r_c the system may more easily circumvent these barriers to adopt energetically favorable conformations.

Structure of the Cryptand. The changes in the energy profile as the Cl^- is moved along r_c are accompanied by distinct changes in the structure of the cryptand. For large separations between the cryptand and the chloride, the ligand is approximately tetrahedral, with the average distance between nitrogen atoms in the vertices of the tetrahedron equal to 5.5 Å. Hydrogen atoms bonded to the nitrogen atoms, H(N), stay in the cryptand cavity, but the N–H(N) bonds do not point straight to the center of the molecule. The average distance from the H(N) atoms to the center is 2.5 Å, and the average distance between two H(N) atoms is 4.0 Å. If the N–H(N) bonds were pointing directly toward the center of the cryptand, the corresponding distances would be 2.3 and 3.7 Å. Since the H(N) atoms carry positive partial charges, the observed increase in the distances between these atoms permits a reduction of electrostatic repulsion and, therefore, is energetically

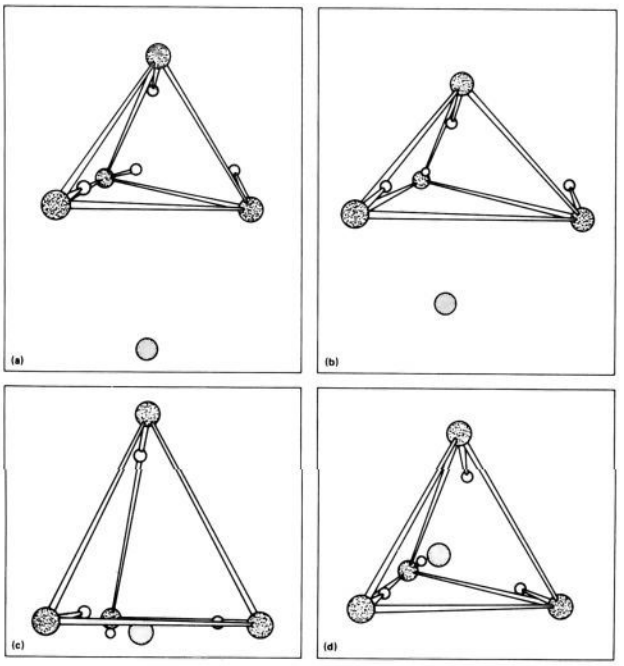

Figure 5. Schematic representation of typical cryptand conformations at r_c = 4.4 Å (a), r_c = 2.9 Å (b), r_c = 2.0 Å (c), and r_c = 0.2 Å (d). Only the nitrogen atoms in the corners of the tetrahedrons with their attached hydrogen atoms and the Cl^- are drawn.

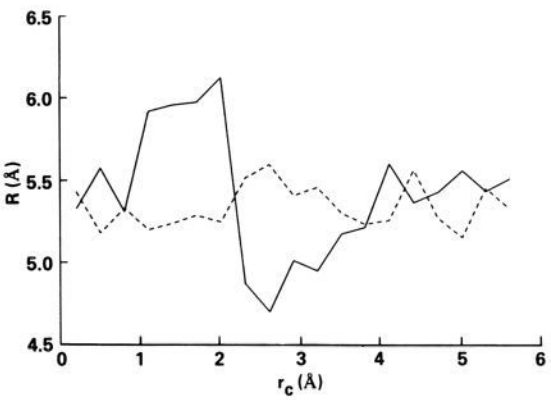

Figure 6. Average distances between the nitrogen atoms in the vertices of the cryptand face directed toward the Cl^- (dashed line) and between these nitrogen atoms and the nitrogen atom farthest away from the Cl^- (solid line) as functions of r_c. Statistical uncertainties are approximately ±0.08 Å.

favorable. The repulsion between the H(N) atoms is obvious in a typical conformation of the cryptand for r_c = 4.4 Å, which is schematically shown in Figure 5a. A similar structure was observed in our calculations of the hydrated cryptand without the presence of chloride.[8]

As the chloride moves toward the ligand from r_c = 4.0 to r_c = 2.6 Å, small but well-defined changes in the cryptand conformation are observed. As shown in Figure 6, the nitrogen atoms, which are in the vertices of the cryptand face nearest to the chloride, N_i (i = 1–3), gradually move apart as r_c decreases. Simultaneously, the distances between these nitrogen atoms and the nitrogen atom farthest away from the Cl^-, N*, are systematically reduced. As a consequence, the cryptand adopts a contracted conformation in which the average distance between N* and N_i is 0.8 Å shorter than that in the tetrahedron. Such a contracted cryptand, with the chloride ion at r_c = 2.6 Å, is shown in Figure 5b. Note that the cryptand contraction increases the free space between the three nitrogen atoms closest to the chloride, reducing steric hindrance during anion transfer into the ligand cavity.

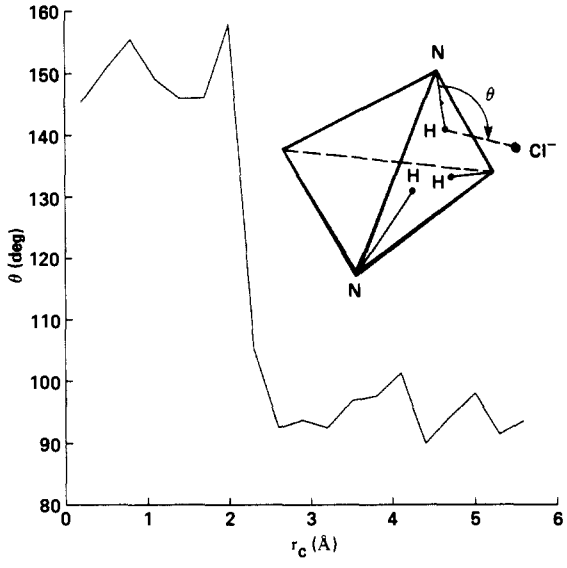

Figure 7. Average angle formed between the Cl^-–$H(N_i)$ and N_f–$H(N_i)$ vectors θ, as a function of r_c. Statistical uncertainties are approximately ±3°.

The cryptand contraction does not markedly affect the directions of the N–H bonds. They stay inside the ligand cavity, and the distances between the H(N) atoms remain virtually unchanged. Similarly, the average angle formed between the Cl^-–$H(N_i)$ and N_f–$H(N_i)$ vectors, shown in Figure 7, stays approximately constant. This angle is close to 90°, indicating that the chloride moves toward the cryptand perpendicularly to the N_f–$H(N_i)$ bonds.

Chloride movement from r_c = 2.6 Å to r_c = 2.0 Å induces dramatic structural changes in the cryptand. In this region, when the chloride encounters the energy barrier, all three N_f–$H(N_i)$ bonds rapidly shift from the inside of the molecule toward the chloride. These new orientations of the N_f–$H(N_i)$ bonds deviate from the pure endo orientation. The corresponding cryptand conformation is shown in Figure 5c. Comparison of this conformation with the structure in Figure 5b clearly demonstrates the extent of changes in the positions of the $H(N_i)$. Another indicator of the observed conformational changes is the average Cl^-–$H(N_i)$–N_i angle. As seen in Figure 7, this angle rapidly increases from 90° to 160°. This means that Cl^-, $H(N_i)$, and N_i are positioned approximately along a straight line and the negative charge on the chloride is located much closer to the positively charged hydrogen atoms. Between r_c = 2.6 and r_c = 2.0 Å the average $H(N_i)$–Cl^- distance decreases from 3.7 to 2.0 Å.

The large observed shifts in the positions of the $H(N_i)$ are accompanied by other structural changes in the cryptand, which indicate the cooperative nature of the conformational transition. Distances between N* and the remaining nitrogen atoms increase by 1.4 Å, while the distances between two N_i atoms simultaneously decrease, on average, by 0.4 Å. The asymmetry in distances between the nitrogen atoms reaches 0.9 Å at r_c = 2.0 Å. This indicates that the cryptand undergoes a rapid transition from the contracted to an elongated conformation. Examples of the internal degrees of freedom that are strongly affected by this cooperative conformational transition are the O–C(O)–C(N_i)–N_i torsional angles in the linkages between N* and N_i, which increase from 25° to 150°. However, not all torsional angles are affected by the transition. For example, other O–C(O)–C(N)–N angles remain nearly unchanged.

Further movement of the chloride toward the center of the cryptand is associated with a conformational relaxation, leading to a structure similar to that of the free ligand. At r_c = 1.1 Å, the O–C(O)–C(N_i)–N_i torsional angles return to the value of 25°. All distances between nitrogen atoms slowly relax to 5.5 Å, and the cryptand again becomes tetrahedral at r_c = 0.2 Å. A relaxed configuration of the cryptand with the anion in the middle is presented in Figure 5d. In the whole range of r_c between 2.3 and 0.2 Å, the average N_f–$H(N_i)$–Cl^- angle, shown in Figure 7,

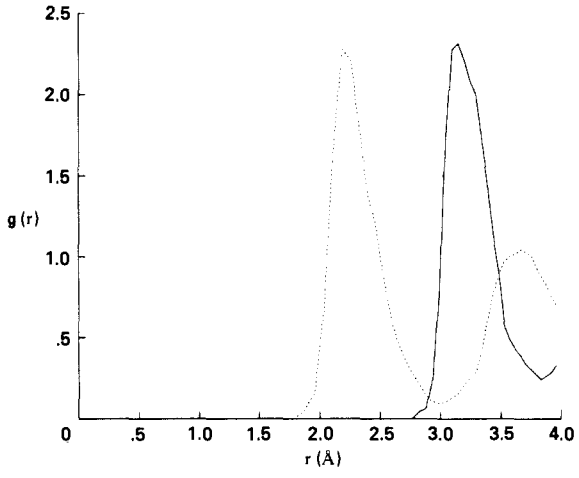

Figure 8. Chloride–water radial distribution functions at r_c = 5.6 Å. The solid line is the Cl^-–O distribution function, $g_{clo}(r)$, and the dotted line is the Cl^-–H distribution function, $g_{clh}(r)$.

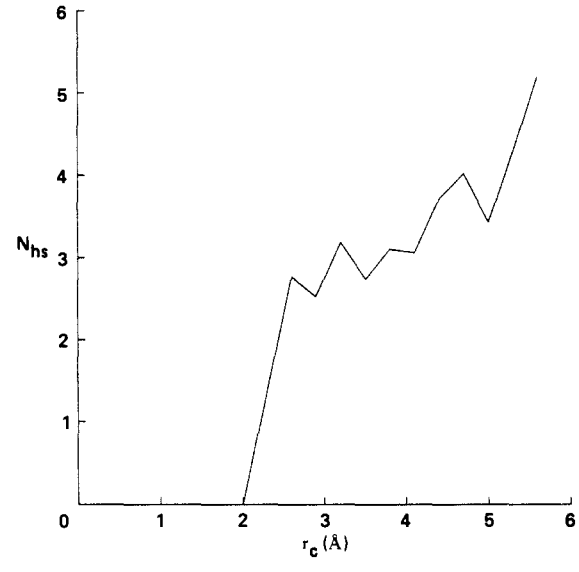

Figure 9. Average number of water molecules in the first hydration shell around chloride, N_{hs}, as a function of r_c.

fluctuates around 150°, demonstrating that the N_f–$H(N_i)$ bonds continue to point toward the Cl^- and guide it into the ligand cavity. The N_f–Cl^-, O–Cl^-, and $H(N_i)$–Cl^- distances change only slightly in this range and are equal to 3.2, 3.5, and 2.4 Å, respectively, when the chloride is located in the ligand cavity. These distances are in a good agreement with the values measured from the crystal structure of the cryptand.[7] They are also close to the corresponding van der Waals distances. Thus, the presence of the chloride ion in the ligand cavity neither creates steric hindrance nor significantly alters the cryptand conformation. The excellent steric fit between these two molecules is a key to explaining the high affinity of cryptand for binding chloride.

Structure of Water. Figure 8 shows radial distribution functions for chloride–water oxygens, $g_{clo}(r)$, and chloride–water hydrogens, $g_{clh}(r)$, when the chloride is located 5.6 Å from the center of the cryptand. This is the maximum anion–ligand separation studied in this work. Both g_{clo} and g_{clh} are similar to the radial distribution functions calculated for dilute aqueous solution of Cl^-.[10] The positions of peaks in $g_{clo}(r)$ and $g_{clh}(r)$ are exactly the same in both cases, suggesting that the orientations of water molecules around the anion are also similar. The main difference in the radial distribution functions between the two systems is in the heights of the first peaks. For the system studied here the peaks are consistently lower due to the presence of cryptand in the neighborhood of chloride. The coordination number, N_{hs}, obtained by integrating the first peak in $g_{clo}(r)$, is equal to 5, while N_{hs} for

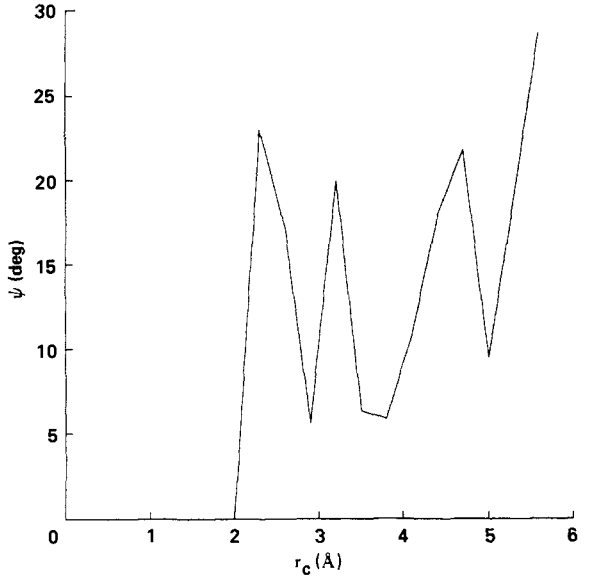

Figure 10. Average angle formed between the coordinate r_c and the line joining N* with the center of the cryptand, ψ, as a function of r_c. Definition of angle ψ is schematically shown in Figure 2.

aqueous solution of Cl^- is 7.3.[10] Thus, even at the largest separation between the chloride and the cryptand studied here, the anion is already partly dehydrated.

Figure 9 shows the dependence of the coordination number on the position of the Cl^- along r_c. As expected, N_{hs} is generally a decreasing function of r_c because the volume around the chloride accessible to water decreases when the anion approaches the cryptand. Note however, that N_{hs} depends nonmonotonically on r_c. This irregular behavior of N_{hs} is related to the direction from which the chloride approaches the cryptand. To examine the anion approach, we monitored ψ, which is the angle between r_c and the line joining N* with the center of the cryptand (see Figure 2). The dependence of ψ on r_c is shown in Figure 10 and is closely correlated with the behavior of N_{hs}. For some values of r_c, the chloride is most often located close to the center of a cryptand face, at equal distances from all three N_i atoms. This orientation of the Cl^- corresponds to ψ close to 0°. For other values of r_c, the chloride is close to an edge joining two nitrogen atoms or close to one of the N_i atoms, and then ψ is approximately 20°. In this case the chloride is more accessible to water and, therefore, N_{hs} is larger than when the anion is near the middle of the cryptand face.

To test the significance of the correlations between r_c and ψ or N_{hs}, we selected two configurations from the trajectory for r_c = 3.2 Å and from the trajectory for r_c = 3.5 Å. These configurations correspond to the extreme instantaneous values of ψ for a given value of r_c. The difference between these extreme values was about 10°. Then, four trajectories 25 ps long were obtained for every configuration by initiating velocities at random from the Maxwell–Boltzmann distribution. For every value of r_c statistical averages of ψ taken from the last 15 ps of every trajectory were identical within statistical errors and were similar to the average from the long trajectory. This result suggests that irregular variations of ψ with r_c are not artifacts of starting conditions.

Water structure is perturbed not only by the presence of chloride but also by the cryptand. Structural changes in water induced by the ligand can be characterized by radial distribution functions of water molecules around the cryptand center. These distribution functions for the chloride placed inside the cryptand and for the free cryptand[8] are shown in Figure 11. In both cases the positions of peaks are identical and are very close to the positions of the peaks when chloride is located outside the ligand. The similarities in the distribution functions indicate that the structure of water around the cryptand is only slightly affected by the presence of Cl^-. The first peaks in the radial distribution functions are associated with water molecules approaching the cryptand through

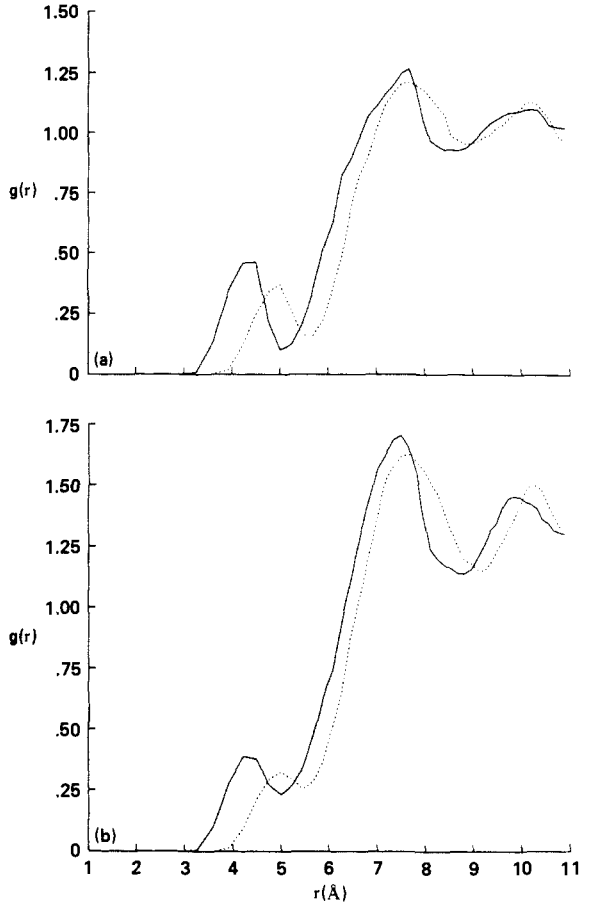

Figure 11. Radial distribution of water molecules around the cryptand center when the chloride is located in the ligand cavity (a) and in the absence of Cl^- (b). The solid line is the center-oxygen distribution function and dotted line is the center-hydrogen distribution function.

its faces, while the second peaks are mostly due to water molecules tightly bound to the $N-H(CH_2)_3$ groups in the vertices of the ligand. The orientations of the water molecules are such that oxygen atoms are close to the positively charged atoms of the cryptand while hydrogen atoms are directed toward the oxygen atoms of the ligand. As a result, the peak in the hydrogen–cryptand center radial distribution function is shifted slightly outward from the peak in the oxygen–cryptand center distribution function.

The positions of the second peaks in the radial distribution functions allow us to estimate the range of perturbations of water structure caused by the cryptand. These peaks are located between 9.5 and 10 Å from the ligand center. The fact that the radial distribution functions in Figure 11b still have a value of about 1.25 at 10.86 Å and continue to decrease indicates that the perturbations extend over the whole simulation box.

Energetic Analysis. Analysis of the energy contributions to U_{tot} provides another viewpoint for examining anion capture by the cryptand, complementing the structural picture presented above. The total energy of the system can be divided into three terms (eq 2) where U_s is the energy of the solute, which consists of the

$$U_{tot} = U_s + U_{sw} + U_w \quad (2)$$

cryptand and the anion, U_{sw} is the energy of interaction between the solute and water molecules, and U_w is the energy of interaction between all water molecules in the system.

A graphical representation of the three components of U_{tot} as a function of r_c is shown in Figure 12. Changes in U_s and U_w favor anion capture while changes in U_{sw} oppose it. At a general level these energy changes can be given a simple explanation. As the Cl^- approaches the cryptand, electrostatic attraction between these two oppositely charged molecules increases and stabilizes the system by lowering U_s. The accompanying process of anion dehydration leads to reduction of the chloride–water interactions

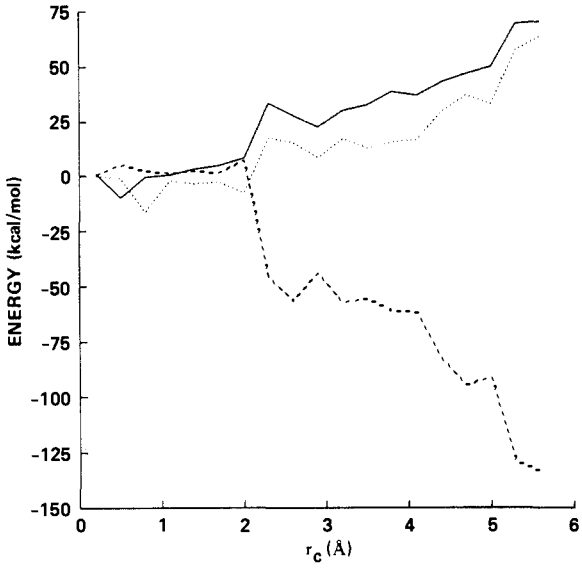

Figure 12. Components of the potential energy of the system, U_{tot}, as functions of r_c. The dotted line is the energy of the solute, which consists of the cryptand and the chloride ion, U_s. The dashed line is the energy of interaction between the solute and water, U_{sw}. The solid line is the energy of interaction between water molecules, U_w. The curves were shifted such that the energies at r_c = 0.2 Å are equal to zero. Statistical uncertainties are typically ±4 kcal/mol for U_s, ±8 kcal/mol for U_{sw}, and ±10 kcal/mol for U_w.

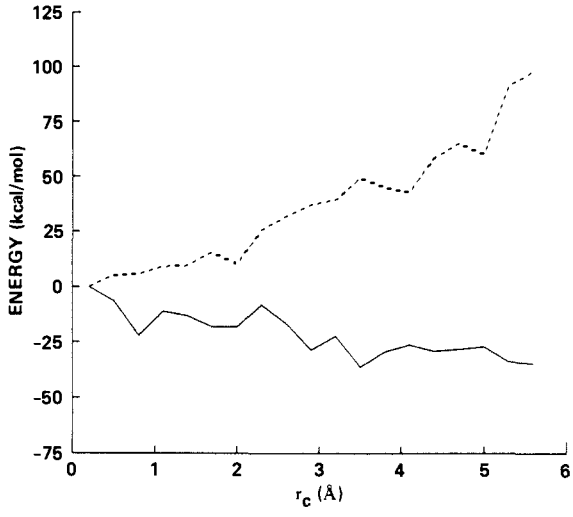

Figure 13. Intrinsic potential energy of the cryptand, U_{cr} (solid line), and energy of interaction between the cryptand and the chloride, U_{crcl} (dashed line), as functions of r_c. The curves were shifted such that the energies at r_c = 0.2 Å are equal to zero. Statistical uncertainties are approximately ±4 kcal/mol.

and, hence, to an increase of U_{sw}. During dehydration, water molecules are successively moved from the vicinity of the Cl^- to the bulk water, where they are able to interact more favorably with other water molecules. Thus, the accompanying changes in U_w favor anion capture.

A detailed analysis of the three contributions to U_{tot} yields further information about the mechanism of chloride capture. The solute energy, U_s, can be partitioned into two terms (eq 3) where

$$U = U_{cr} + U_{crcl} \quad (3)$$

U_{cr} is the intrinsic energy of the cryptand and U_{crcl} is the energy of interaction between the cryptand and the chloride. These two terms, shown in Figure 13, contribute oppositely to U_s.

Changes in U_{cr} oppose anion capture and are closely correlated with the changes in the distances between the $H(N_i)$ atoms. For large values of r_c, where orientations of the $H(N_i)$ atoms remain approximately constant, U_{cr} changes only slightly. Between r_c = 2.6 and r_c = 2.0 Å, the positively charged $H(N_i)$ atoms shift

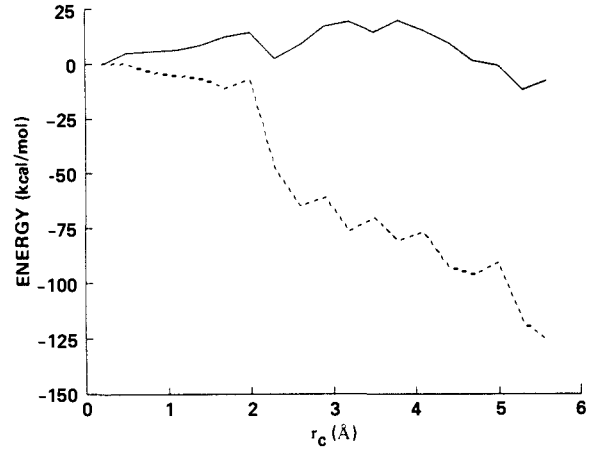

Figure 14. Energy of interaction between cryptand and water, U_{crw} (solid line), and energy of interaction between chloride and water, U_{clw} (dashed line), as functions of r_c. The curves were shifted such that the energies at r_c = 0.2 Å are equal to zero. Statistical uncertainties are approximately ±6 kcal/mol.

outside of the cryptand and the distances between them markedly decrease. These conformational changes lead to the increase in electrostatic repulsion contributing to U_{cr}. Also, in this range of r_c we observe a rapid increase in the contributions to U_{cr}, which represent deformations of bonds and angles of the cryptand. These unfavorable energy changes, equal to 10 kcal/mol, indicate the existence of the conformational strain temporarily induced in the cryptand to accommodate the entering chloride.

In contrast to U_{cr}, changes in U_{crcl} favor anion capture, mostly due to the increase in electrostatic attraction between the chloride and the cryptand. The largest change in U_{crcl} occurs between r_c = 2.6 Å and r_c = 2.0 Å, when the $H(N_i)$ atoms move to the outside and approach the chloride. This change is partly electrostatic in nature. However, it also includes steric repulsion of 10 kcal/mol, which is due to the hindrance encountered by the chloride as it moves through a face of the cryptand. As the Cl^- moves further into the cage, the electrostatic contribution to U_{crcl} changes only slightly because the $H(N_i)$ bonds move with the chloride toward the center of the ligand and the $H(N_i)$–Cl^- distance stays virtually the same. Simultaneously, the repulsive steric contribution to U_{crcl} is slowly reduced and approaches 1 kcal/mol when the chloride is located in the center of the cryptand. Such low repulsion energy provides evidence for the excellent steric fit between the cryptand and the chloride.

The remaining two terms in eq 2, U_{sw} and U_w, describe energetic aspects of the anion dehydration and accompanying changes in water structure. U_{sw} is a sum of two terms (eq 4) where U_{crw} is

$$U_{sw} = U_{crw} + U_{clw} \quad (4)$$

the energy of interaction between the cryptand and water and U_{clw} is the energy of interaction of the chloride with water. For convenient analysis U_w can be expressed as a sum of the energies of each water molecule in the system (eq 5) where U_i is the energy

$$U_w = \sum_i U_i \quad (5)$$

of interaction of water molecule i with all other water molecules and is defined as in eq 6 where U_{ij} is the energy of interaction between water molecules i and j.

$$U_i = \tfrac{1}{2}\sum_{j \neq i} U_{ij} \quad (6)$$

Both components of U_{sw} in eq 4 are shown in Figure 14. As can be seen, changes in U_{sw} are mostly associated with U_{clw}. U_{crw} changes much less than U_{clw}, in agreement with our previous evidence that water molecules around the cryptand are rigidly bound and are not strongly influenced by the presence of chloride.

At the largest separation between the cryptand and the anion studied here, U_{clw} is equal to −74 kcal/mol, which is about half of the chloride–water energy in the dilute aqueous solution of Cl^- calculated with the same cutoffs.[8] Between r_c = 5.6 Å and r_c =

2.6 Å U_{clw} increases in a stepwise manner. This increase is closely correlated with the changes in N_{hs}, shown in Figure 9. For every water molecule removed from the immediate vicinity of the anion, U_{clw} increases by about 18 kcal/mol. Approximately half of this increase comes from the change in the energy of interactions between the chloride and the neighboring water molecules. The other half is associated with the energy changes between Cl^- and water molecules beyond its first hydration shell.

The increase of U_{clw} due to anion dehydration is partially compensated by the decrease of U_w. Between r_c = 5.6 Å and r_c = 2.6 Å, U_w changes by −39 kcal/mol. One reason for this decrease is that the average U_i of a water molecule in the first hydration shell around the chloride is about −6.5 kcal/mol, while the average U_i of the remaining water molecules is −9.4 kcal/mol. Thus, the two water molecules moved from the vicinity of the anion to the bulk water contribute −5.8 kcal/mol to U_w. The remaining decrease in U_w, equal to −33 kcal/mol, can be attributed to the energetically favorable rearrangement of water structure.

As the chloride moves from r_c = 2.6 Å to r_c = 2.0 Å, the remaining three water molecules from its hydration shell are lost. Simultaneously, U_{clw} rapidly increases to 40 kcal/mol for a completely dehydrated ion, indicating that interactions between Cl^- and water become repulsive. A detailed analysis of water structure indicates that U_{clw} becomes positive because water molecules around the cryptand are oriented in such a way that their interactions with the positively charged $N-H(CH_2)_3$ groups are optimal. Such orientations of water molecules lead, in turn, to unfavorable interactions with the negatively charged chloride. These interactions are unchanged as the Cl^- moves toward the center of the cryptand and, consequently, U_{clw} remains positive. Accompanying changes in U_w are less pronounced. As is true for larger values of r_c, the decrease in U_w between r_c = 2.6 Å and r_c = 2.0 Å partially compensates the changes of U_{clw}. When the chloride moves further into the cryptand, water–water interactions do not change appreciably.

Origin of the Energy Barrier. A significant feature of chloride capture by the cryptand is the presence of an energy barrier to movement of the anion from the outside and the inside of the ligand. The structural and energetic analysis presented above allows us to understand better the origin of this barrier.

There are two factors that contribute to the barrier. One is the steric hindrance experienced by the chloride as it enters the cryptand, which accounts for approximately 10 kcal/mol in the energy increase. The second contribution to the barrier is due to dehydration of the anion. This process is associated with a significant increase of U_{clw} that is only partially compensated for by the decrease of U_w. The net effect of the dehydration process is approximately 40 kcal/mol.

The two energy contributions discussed above are sufficiently large that they would prohibit effective chloride transfer across the barrier. Thus, they must be balanced by a favorable contribution that lowers the energy barrier. This contribution comes from a conformational transition of the cryptand in which the N_f–$H(N_f)$ bonds shift toward the chloride. Electrostatic attraction between Cl^- and $H(N_f)$, which increases during the transition, reduces the barrier for anion binding by about 30 kcal/mol.

The concept that the shift of the $H(N_f)$ atoms is essential for the effective chloride transfer into the cryptand raises a question about the size of the energy barrier to anion capture if the shift did not occur. This question was answered by obtaining a molecular dynamics trajectory at r_c = 2.3 Å in which the cryptand did not undergo the conformational transition but rather was trapped in a local minimum corresponding to the $H(N_f)$ atoms located inside the ligand. When the chloride was moved further toward the center of the cryptand, the shift of the N_f–$H(N_f)$ bonds could not occur because it would cause a large steric interference between the $H(N_f)$ and the Cl^-. This data explains why the conformational transition in the cryptand occurs normally in a narrow range of r_c before Cl^- gets too close to the ligand.

The energy profile for the alternative pathway of chloride capture is shown in Figure 15. The energy barrier is rather steep with the maximum at r_c = 1.8 Å and is about 30 kcal/mol higher

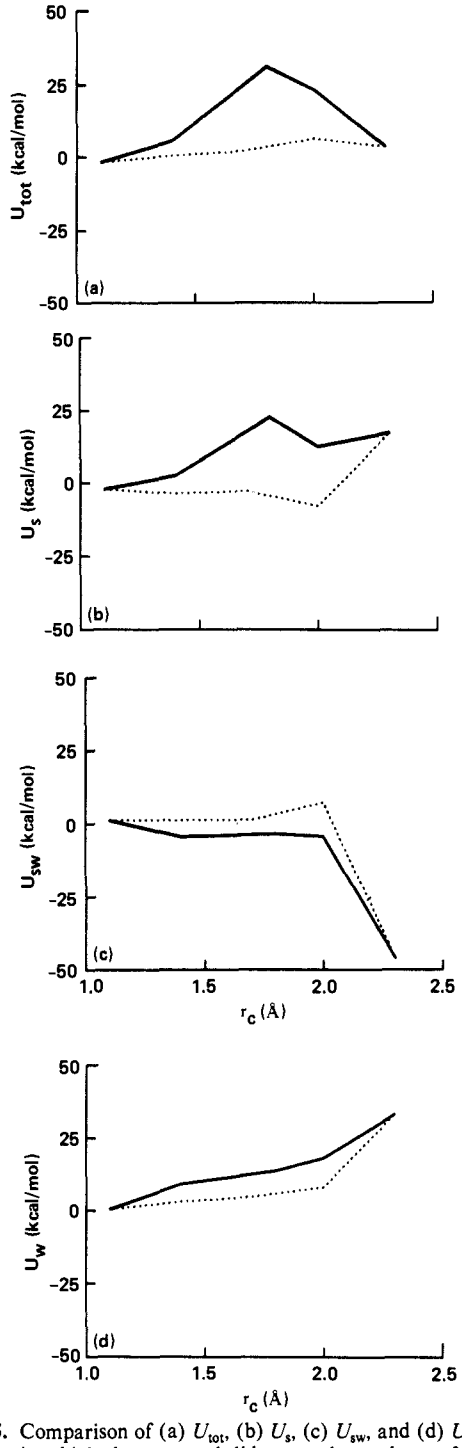

Figure 15. Comparison of (a) U_{tot}, (b) U_s, (c) U_{sw}, and (d) U_w between the system in which the cryptand did not undergo the conformational transition (solid line) and the system in which the cryptand underwent the transition (dotted line).

than the barrier in the energy profile shown in Figure 4a. When the chloride is moved further into the cryptand, the difference between both energy curves decreases, as expected, because both pathways should eventually lead to the same complex of the chloride trapped inside the cryptand. Comparison of energy contributions to U_{tot} shows that the energy term that differs most is U_s. The difference is mainly due to the electrostatic component of chloride–cryptand interactions. This result supports the conclusion that the shift of N_f–$H(N_f)$ bonds and electrostatic stabilization associated with this conformational change play a crucial role in decreasing the energy barrier and facilitating chloride capture.

The discussion of the barrier presented here is limited to the energy component only. It would appear that our calculations

should be sufficient to obtain also entropic contribution to the barrier by one of thermodynamic perturbation strategies[17] using r_c as the integration parameter. All these strategies require serial comparisons of similar states of the system. This condition is difficult to fulfill between r_c = 2.6 Å and r_c = 2.0 Å. Since the shifts of the N_i–H(N_i) bonds in this range of r_c are rapid, we were not able to locate such values of r_c that correspond to the equilibria between the two orientations of each bond. Thus, free energy differences in this region calculated by simple integration over r_c would be unreliable. Different perturbation approach to calculating these free energy differences is currently under study.

Conclusions

The process of chloride capture by the cryptand exhibits several characteristic features. The receptor has two binding sites in which the anion is located inside the ligand cavity or is loosely bound outside the cryptand. The corresponding energy minima are separated by a barrier of approximately 20 kcal/mol. Chloride capture is accompanied by a stepwise dehydration of the anion. The loss of hydration energy associated with the removal of water molecules surrounding Cl^- is offset by electrostatic attraction between the positively charged cryptand and the negative chloride.

The most striking features of chloride capture are rapid changes of virtually all of the energetic and structural parameters characterizing this process that occur in a very narrow range of r_c between 2.6 and 2.0 Å. In this range the chloride ion loses the last three water molecules from its first hydration shell and starts moving through a face of the cryptand into the intramolecular cavity. Large cooperative conformational changes compensate for the loss of favorable chloride–water interactions and reduce steric hindrance. During the conformational transition, the overall molecular shape of the ligand changes and three N–H bonds close to the anion move from the intramolecular cavity to point toward the chloride. This new conformation provides electrostatic stabilization that greatly reduces the energy barrier. The three bonds move with the anion in its further progression toward the center of the cryptand. It appears that chloride perfectly fits the ligand cavity. The distances between the Cl^- and the nitrogen and oxygen atoms of the cryptand are very close to the corresponding van der Waals radii, and the substrate–ligand repulsion energy is low. The conformation of the free cryptand is similar to that of the cryptate, indicating that large steric adjustments are not necessary to accommodate the anion.

The description of chloride capture presented above underscores an important, general requirements for both efficient and selective ion binding by an ionophore. A good receptor must have a structure that properly balances rigidity and flexibility. Structural rigidity is needed to ensure selectivity in substrate binding. For instance, computer simulation studies[18] showed that free energy of binding Cl^- by the cryptand is 3.2 kcal/mol lower than free energy of binding Br^- because the bromide ion cannot be easily accommodated in the ligand cavity. On the other hand, molecular flexibility is necessary to reduce the energy barrier to ion capture. For one of the best studied ion-transporting molecules, gramicidin A, it has been shown that the flexibility of the ethanolamine end considerably influences the energy profiles of ion capture close to the entrance of the channel.[19] In the same study progressive dehydration of Na^+ and the competition between different energy terms was similar to that observed here.

The reduction of energy barrier to ion capture by the cryptand is due to strong, favorable electrostatic interaction between the chloride and positively charged groups of the receptor. Similar mechanisms have been implicated in chloride binding by $GABA_A$ receptor.[20] It was found that positively charged amino acid side chains cluster in the mouth of the ion channel. These residues may not only act simply as an anion-selective filter but also actively assist chloride dehydration in a similar way as do the N–H groups of the cryptand. These similarities suggest that general features of ion capture discussed here may be characteristic of a broad range of both biological and abiotic ion receptors.

Acknowledgment. This work was supported by NASA—University Consortium Interchange No. NCA2-108. We thank Dr. Andrew Komornicki for providing his GRADSCF program and for discussions of ab initio calculations. The computer facilities used in this work were provided by the Numerical Aerodynamic Simulation (NAS) program.

Registry No. H_2O, 7732-18-5; Cl^-, 16887-00-6; Cryptand SC24, 56698-26-1.

(17) See e.g.: Pohorille, A.; Pratt, L. R. *Methods Enzymol.* **1986**, *127*, 64.

(18) Lybrand, T. P.; McCammon, J. A.; Wipff, G. *Proc. Natl. Acad. Sci. U.S.A.* **1986**, *83*, 833.

(19) Etchebest, C.; Pullman, A. *J. Biomol. Struct. Dyn.* **1986**, *3*, 805.

(20) Schofield, P. R.; Darlison, M. G.; Fujita, N.; Burt, D. R.; Stephenson, F. A.; Rodriguez, H.; Rhee, L. M.; Ramachandran, J.; Reale, V.; Glencorse, T. A.; Seeburg, P. H.; Barnard, E. A. *Nature (London)* **1987**, *328*, 221.